Published in: American Society for Mass Spectrometry (2006), vol.17, pp.180-188
Status: ¨Postprint (Author's version)

Monitoring the Zinc Affinity of the Metallo-β-Lactamase CphA by Automated nanoESI-MS

Kris De Vriendt, Gonzalez Van Driessche, Bart Devreese[1], Carine Bebrone, Christine Anne, Jean-Marie Frère, Moreno Galleni[2], Jozef Van Beeumen[3]

[1] *Laboratory of Protein Biochemistry and Protein Engineering, Ghent University, Ghent, Belgium*
[2] *Centre d'Ingénierie des Protéines, Institut de Chimie B6, Université de Liège, Liège, Belgium*
[3] *Laboratory of Protein Biochemistry and Protein Engineering, Ghent University, Ghent, Belgium*

Abstract

Metallo-*β*-lactamases are zinc containing enzymes that are able to hydrolyze and inactivate *β*-lactam antibiotics. The subclass B2 enzyme CphA of *Aeromonas hydrophila* is a unique metallo-*β*-lactamase because it degrades only carbapenems efficiently and is only active when it has one zinc ion bound. A zinc titration experiment was used to study the zinc affinity of the wild-type and of several mutant CphA enzymes. It shows that a second Zn^{2+} is also bound at high ion concentrations. All samples were analyzed using mass spectrometry in combination with an automated nanoESI source. The metal-free enzyme has a bimodal charge distribution indicative of two conformational states. A completely folded enzyme is detected when the apo-enzyme has bound the first zinc. Intensity ratios of the different enzyme forms were used to deduce the zinc affinities. CphA enzymes mutated in metal ligands show decreased zinc affinity compared to wild-type, especially D120 mutants.

Beta-lactamases play a key role in bacterial resistance by hydrolyzing and thus inactivating *β*-lactam antibiotics, the most important group of clinically used antibiotics. They have been divided into four classes (A to D) according to the Ambler classification; serine-*β*-lactamases constitute classes A, C, and D, while enzymes of class B contain metallo-*β*-lactamases [1, 2]. The latter are metallo-enzymes exhibiting full activity with Zn^{2+} as cofactor. They are of clinical importance as they can hydrolyze all classes of *β*-lactams, including fourth-generation cephalosporins and carbapenems. Moreover, the enzymes are insensitive to available *β*-lactamase inhibitors, such as clavulanic acid. Metallo-*β*-lactamases have been described in a number of environmental species, but are also found in clinical isolates such as *Burkholderia cepacia, Pseudomonas aeruginosa, Stenotrophomonas maltophilia* and some Enterobacteriaceae [3]. Their increasing occurrence and rapid dissemination by horizontal gene transfer has boosted clinical and biochemical studies in the past few years. Three subclasses of metallo-*β*-lactamases, B1 to B3, have been described [4]. The three-dimensional structures of the subclass B1 enzymes BcII and CcrA show the presence of two zinc ions in the active site [5, 6]. The first zinc ion is tetrahedrally coordinated by three histidine residues (H116, H118, and H196) and a water molecule. The second zinc ion is stabilized by D120, C221, H263, and two water molecules in a trigonal-bipyramidal geometry. One water molecule acts as a bridge between the two zinc ions, serving as ligand for both atoms. We will refer to these two binding sites as the histidine site and the cysteine site, respectively. In subclass B3, three-dimensional structures are solved for Fez-1 and L-1 [7, 8]. These structures show a histidine-site identical to that of subclass Bl, but a modified cysteine site where D120, H121, and H263 coordinate the second zinc ion. C221 is replaced by a serine, but this residue does not participate in zinc binding. On the basis of sequence alignments the potential zinc ligands for the B2 enzyme CphA of *Aeromonas hydrophila* were initially predicted to be N116, H118, and H196 for the histidine site and D120, C221, and H263 for the cysteine site [4, 9]. However, X-ray crystallography recently showed that the first zinc ion is located in the cysteine site instead of in the histidine site [10]. Moreover, unlike the other class B enzymes, CphA is only active as a mono-zinc protein. Moreover, the enzyme has a narrow substrate profile, with only carbapenems being hydrolyzed efficiently [11].

In this work, we used a nanoESI-MS platform for the characterization of CphA. The platform consists of a Q-TOF instrument interfaced to the automated nanoESI source NanoMate 100 (Advion Biosciences, Ithaca, NY).

In this new system, samples are automatically picked up from a 96-well plate using conductive spraying tips and are electro-sprayed using a 100 nozzle containing silicon chip, placed in front of the mass spectrometer orifice. The instrument is well described elsewhere [12] and has been successfully used for the analysis of noncovalent protein-protein and protein-nonmetal ligand interactions [13-16]. In the present work, we use it to analyze the zinc affinity of the wild-type CphA enzyme and of several mutated enzymes in a semi-high throughput fashion. Metal-free enzyme was prepared and subjected to zinc titration. The titration method allows following the

accumulation of mono-zinc and di-zinc enzymes according to the scheme:

$$\mathrm{Apo-E + Zn \rightleftharpoons E-Zn + Zn \rightleftharpoons E-Zn_2} \qquad (1)$$

Important advantages of mass spectrometry over many other analytical methods are its sensitivity (and thus low sample consumption) and the possibility to detect different species simultaneously. NanoESI-MS has been used previously for studying metallo-peptide and metallo-protein complexes [17-20]. Following the recent description on the use of the chip-based nanoESI source in monitoring the activity of metallo-enzymes by van den Heuvel et al. [21], this work reports the characterization (metal constitution, stoichiometry, and affinity) of metallo-proteins using this nanoESI device.

Materials and Methods

Chemicals

Ammonium acetate (NH_4OAc) and ethylenediami-netetraacetic acid (EDTA) were purchased from Sigma-Aldrich (St. Louis, MO). Zinc acetate ($Zn(OAc)_2$) was obtained from Fluka (Buchs, Switzerland). All buffers and solutions were prepared in Milli-Q water (Millipore, Bedford, MA).

Preparation of Metal-Free Enzyme

CphA wild-type and mutant proteins were expressed and purified as described [22]. Apo-enzyme was prepared by incubating the protein with 10- to 20-fold molar excess of EDTA for 1.5 h at room-temperature. The excess EDTA was removed by an overnight dialysis against 10 mM NH_4OAc, pH 6.8, using mini-GebaFlex tubes (GeBa, Rfar-Hanagid, Israel). The protein concentration was determined using a ε_{280nm} of 37,500 $M^{-1}cm^{-1}$.
A 1 mM $Zn(OAc)_2$ stock solution was prepared in 10 mM NH_4OAc, pH 6.8. The titration experiment was performed by mixing the protein with 0 to 100 μM Zn^{2+}.

Nanoelectrospray Ionization Mass Spectrometry (nanoESI-MS)

Denatured proteins, at a concentration of 1 μM, were ionized from a solution containing 50% acetonitrile and 0.1% formic acid. For native measurements, all samples were prepared to a final concentration of 9 to 10 μM (in 10 mM NH_4OAc, pH 6.8) in triplicate, except for CphA K228Q, for which each sample was analyzed only once. All samples were analyzed using nanoESI-MS on a Q-TOF1 mass spectrometer (Micromass, Manchester, UK) equipped with a NanoMate 100 device (Advion Biosciences). The system was set to the automatic infusion mode using a contact closure signal between the NanoMate 100 and the mass spectrometer. Spraying parameters were a spraying voltage of 1.8 kV (unless mentioned specifically), a sample pressure of 0.2 to 0.3 psi, a cone voltage of 50 V, a source temperature of 45 °C, and a scan range from 700 to 3200 m/z with a scan time set to 1 s. The 96-well plate was loaded with 5 μL of each sample from which 4 μL was infused for 5 min. An adhesive seal was used to cover the 96-well plate to prevent evaporation of the samples. A new tip was utilized for each sample to prevent cross-contamination. All experimental masses were within 50 ppm of the calculated masses.

Data Processing and K_d Determination

All data were processed using MassLynx software version 3.1. Raw spectra were smoothed. The total intensities of apo-enzyme (E), mono-zinc enzyme (EL), and di-zinc enzyme (EL_2) were calculated by summing the peak height intensities of all charge states, including adduct intensities. Concentrations of E, EL, and EL_2 were determined from the relative intensities and by equalizing the sum of all intensities with the initial enzyme concentration. These concentrations were used to calculate ϑ, the average number of zinc ions bound per molecule of enzyme, using the following equation:

$$\vartheta = \frac{[\mathrm{EL}] + 2[\mathrm{EL_2}]}{[\mathrm{E}] + [\mathrm{EL}] + [\mathrm{EL_2}]} \qquad (2)$$

The ϑ values were plotted as a function of the equivalents of zinc added to the enzyme. From this plot, the dissociation constant $K_{d,1}$ for the first zinc ion and $K_{d,2}$ for the second zinc ion were deduced by calculating the equilibrium zinc concentration at ϑ of 0.5 and 1.5, respectively.

Results and Discussion

Spray Optimization

ESI spray stability is affected by several variables such as the applied voltage, solution, and gas flow rates, distance between capillary and counter electrode, and sample properties. In contrast to pulled capillary needles, the NanoMate 100 device offers the possibility to control most of these variables. For example, the distance between the chip and the cone orifice can be adjusted, but once set, the distance will be the same for every sample. A critical parameter to obtain a stable ESI spray is the voltage applied to generate the charged droplets. Figure 1 shows the TIC chromatograms of native CphA at 1.5, 1.6, 1.7, 1.8, and 1.9 kV. As the voltage increases, a more stable spray is generated. The spray reaches its highest stability at 1.8 kV and decreases again at a higher voltage setting. It is most stable in the cone-jet mode, i.e., when the Taylor cone has a constant shape [23]. The cone-jet mode is achieved at an intermediate voltage when a constant emission of droplets occurs. If the voltage is too low, the Taylor cone collapses after ejecting a stream of droplets. At high voltages, multiple cones can appear, resulting in off-axis droplet formation [24]. On the other hand, a relatively high voltage has to be applied, taking into account the high water content of the samples. Because water has a higher surface tension than organic solvents, higher voltages are necessary to maintain the cone-jet operation. All samples, as described in the next sections, were sprayed at 1.8 kV.

Figure 1: *Total ion current chromatograms of 10 µM wild-type CphA in 10 mM NH_4OAc at a spraying voltage of (a) 1.5 kV, (b) 1.6 kV, (c) 1.7 kV, (d) 1.8 kV, and (e) 1.9 kV.*

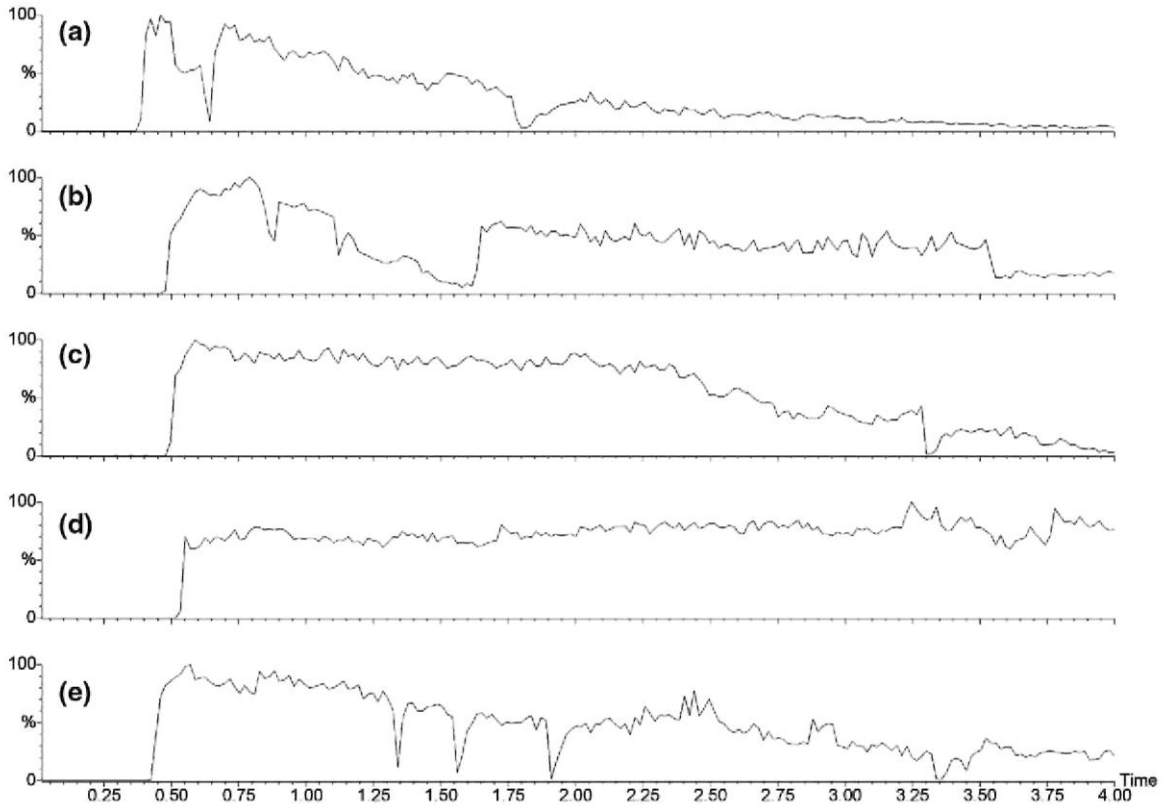

Preparation of Metal-Free Enzyme

Figure 2a and b show the spectra of denatured and native wild-type CphA, respectively. Spectrum b is a typical *m/z* spectrum for a native protein, with only a few charge states being detected at high mass-to-charge values. The deconvoluted spectrum (inset) shows a mass of 25,189 Da for the denatured enzyme and of 25,252 Da for the native enzyme. These values are equal to the theoretical molecular masses. The mass difference between

them (63 Da) fits the mass of one zinc atom (65 Da), the 2 Da difference being the result of a loss of two protons upon binding the metal ion. Figure 2c is the *m/z* spectrum of nondenatured wild-type CphA after complete removal of the zinc atom by EDTA. The spectrum shows a bimodal charge distribution, typical for two populations of species having different conformational states. The first more unfolded population has high charge states (12+ to 27+) similar to the denatured *m/z* spectrum. The second folded population has low charge states (9+ to 11+), as has the native mono-zinc enzyme. This result suggests that the protein is destabilized, most likely unfolded, when the zinc is removed from the active site, at least under the conditions used in this work. On the basis of microcalorimetric and circular dichroism results, Hernandez-Valladares et al. also concluded that the mono-zinc form was more stable and more compact than the apo-enzyme [11]. A similar destabilization was observed using ESI-MS for two other metallo-proteins, the metallo-β-lactamase Bell (our unpublished results) and colicin E9 endonuclease [20].

Figure 2: *Raw mass spectra of mono-zinc wild-type CphA, denatured in 50% acetonitrile/0.1% formic acid (a), native in 10 mM NH_4OAc (b), and metal-free in 10 mM NH_4OAc (c). Insets show the deconvoluted mass spectra.*

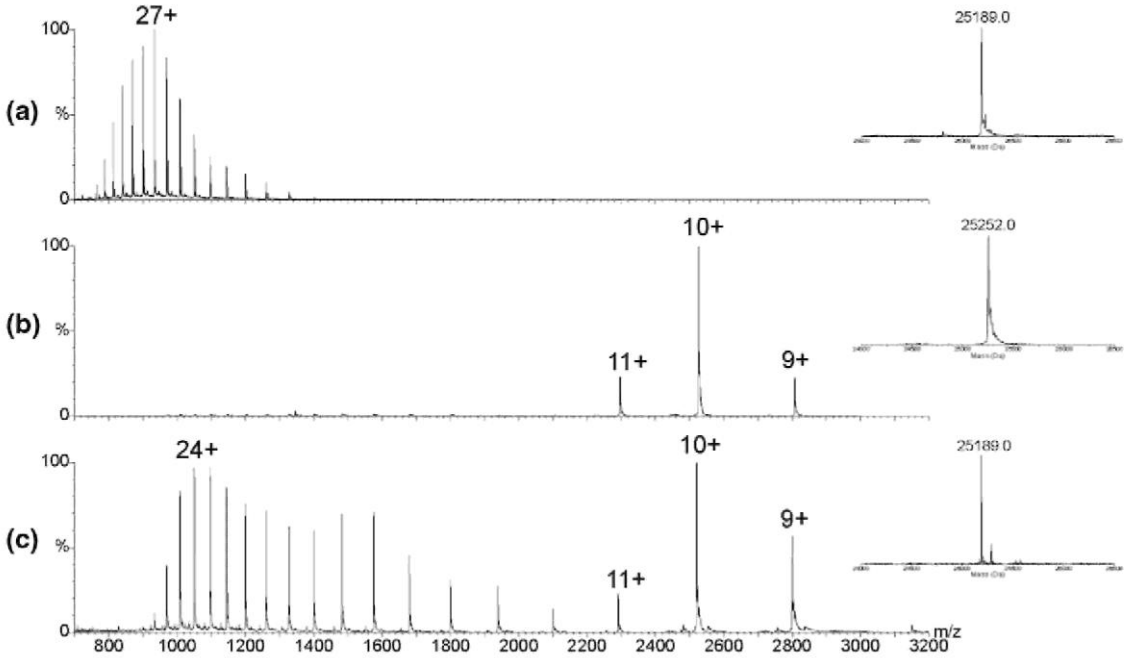

On-Line Monitoring of Zinc Removal by EDTA

Metal chelating agents such as EDTA are able to inactivate metallo-β-lactamases by zinc sequestering. Two possible mechanisms have been proposed [21-24]. The first presumes the formation of a tertiary complex of enzyme:Zn^{2+}:EDTA, while the second presumes a dissociation of the enzyme:Zn^{2+} complex before the zinc is chelated by EDTA. Although inactivation by the latter mechanism is suggested to occur in a few instances [25, 26], the former mechanism is believed to be the more general one [27, 28]. Also, the chelator mediated inactivation of CphA has been proposed to proceed via the formation of a tertiary complex [11]. To verify this proposal, we mixed EDTA (15 μM) with the mono-zinc wild-type enzyme (10 μM) and immediately thereafter infused the mixture into the mass spectrometer. The result in Figure 3 shows spectra at different time points. The abundance of zinc-bound enzyme clearly decreases, while the abundance of apo-enzyme concomitantly increases. As explained in the previous section and illustrated in Figure 2c, a high charge state population is formed when the holo-enzyme is converted to apo-enzyme. The rise in TIC intensity over time (Figure 3) is most likely due to the increasing formation of apo-CphA. Without EDTA, no change in the apo/holo-enzyme ratio could be observed during spraying time. The overall reaction rate appears to be quite high, with 50% of the holo-enzyme being converted to its apo form after 1 min (part b in Figure 3). However, on the basis of the model that seems to prevail under the conditions used in solution, a dissociation rate for the complex of 6×10^{-3} s^{-1} should be expected, indicating a much slower reaction rate [11]. This difference may be explained by assuming that the tertiary complex is unstable in the gas-phase and that it dissociates during its flight to the detector. Alternatively, or in addition, the reaction kinetics in the spraying tip may be influenced by the spraying conditions (high voltage).

Published in: American Society for Mass Spectrometry (2006), vol.17, pp.180-188
Status: ¨Postprint (Author's version)

Zinc Titration of CphA

In the second part of this work, we investigated the affinity for zinc of wild-type CphA using a titration experiment. Titration of the wild-type apo-enzyme with increasing concentrations of zinc ions initially shifts the apo-enzyme to its mono-zinc (Figure 4). At concentrations higher than 40 μM zinc, also the di-zinc forms are visible. The less compact apo-enzyme population disappears completely when the enzyme binds one zinc atom. The unfolding process of the metal-containing enzyme to the metal-free enzyme is thus reversible and the equilibrium between the unfolded and folded state is shifted towards the folded native state when a zinc atom is sequestered. The number of zinc atoms per enzyme (ϑ) was calculated using eq 2, with the concentrations [E], [EL], and [EL_2] being calculated from the intensity ratios E/EL and EL/EL_2, and was plotted versus the equivalents zinc added to the apo-enzyme (Figure 5a). Experimental errors, calculated as coefficients of variation, were within 20%. The wild-type enzyme is completely mono-zinc at 1.5 equivalents of zinc, while the di-zinc enzyme is not formed with less than 3 equivalents. There is still a considerable fraction of mono-zinc enzyme at 7.5 equivalents. $K_{d,1}$ and $K_{d,2}$, the dissociation constants for the first and the second zinc atom can be deduced at a ϑ value of 0.5 (50% mono-zinc enzyme formed) and 1.5 (50% di-zinc enzyme formed), respectively. For the wild-type enzyme, this results in a value for $K_{d,1}$ of 8 μM and of 55 μM for $K_{d,2}$ (Table 1). The dissociation constants for the zinc atoms reported by Hernandez-Valladares et al. are 7 pM and 46 μM, respectively [11]. Although the $K_{d,2}$ determined in this work is only slightly higher than the K_d determined using solution-based techniques, it is remarkable that the dissociation constant for the first zinc atom is a factor 10^6 higher than $K_{d,1}$ determined in solution. With a K_d of 7 pM, the enzyme is expected to be completely mono-zinc at 1 equivalent of zinc. In our work, only 20% mono-zinc enzyme was detected at 1 equivalent of zinc and, as already stated above, a completely mono-zinc enzyme was only reached at 1.5 equivalents of zinc.

Figure 3: *On-line monitoring of the zinc removal by EDTA. Mass spectra a to g are the combined spectra over a period of 30 s. Spectra on the right side show the 10+ charge state and the formation of the apo-enzyme.*

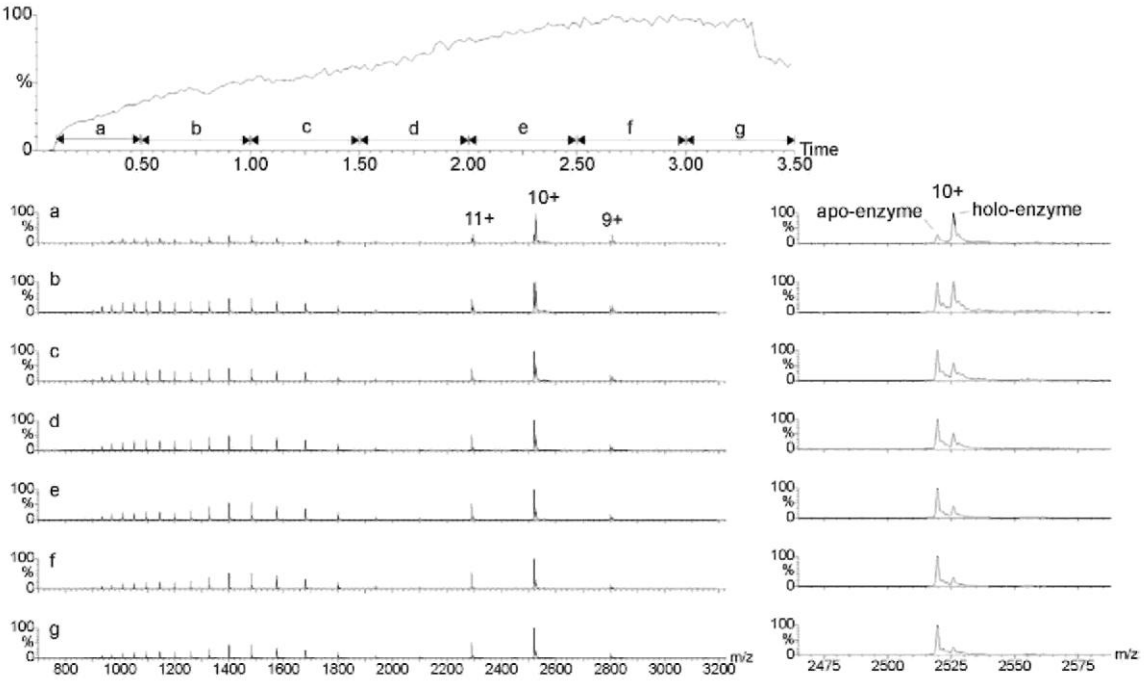

Published in: American Society for Mass Spectrometry (2006), vol.17, pp.180-188
Status: ¨Postprint (Author's version)

Figure 4: *Titration spectra of apo-CphA with 0,10, and 30 µM Zn^{2+}. Peaks labeled with one asterisk and two asterisks are charge states of the apo-enzyme and mono-zinc enzyme, respectively.*

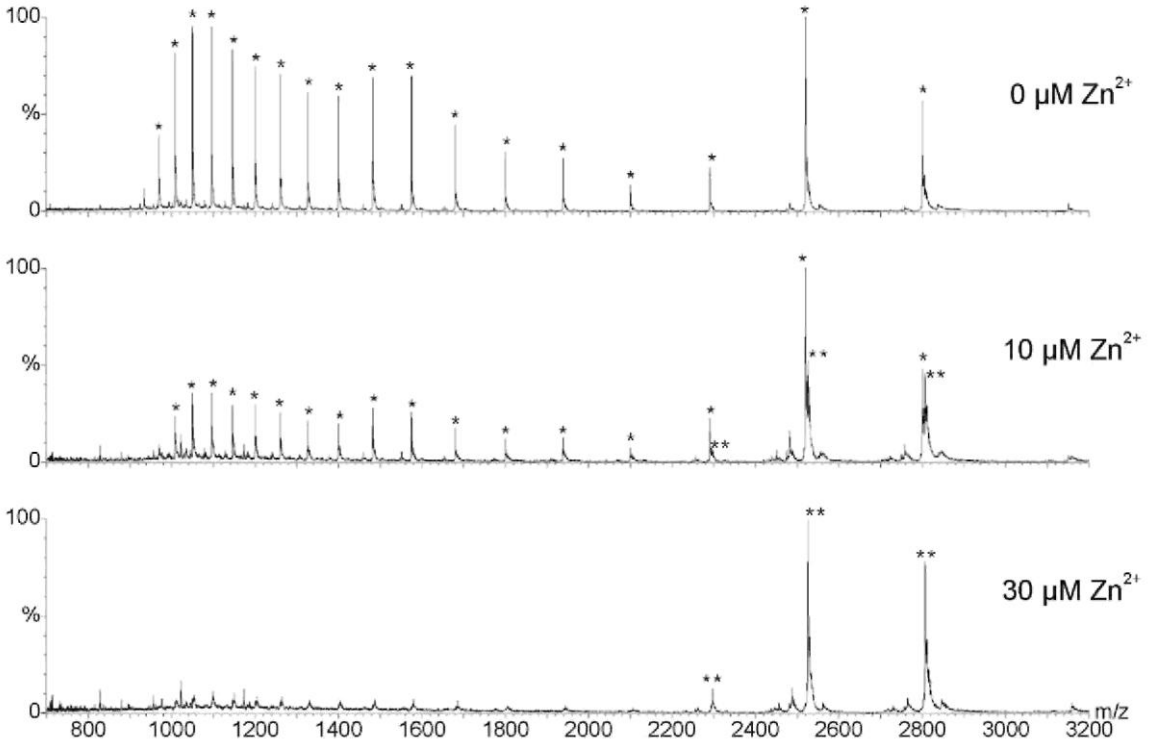

Figure 5: *Titration plot of number of zinc atoms per molecule of enzyme, ϑ, versus equivalents of zinc for wild-type CphA (filled circle), K228Q (open triangle), N116H (open circle), N220G (filled diamond), and N116H-N220G (asterisk) before (a) and after (b) applying the correction factor of 12.5 (see text).*

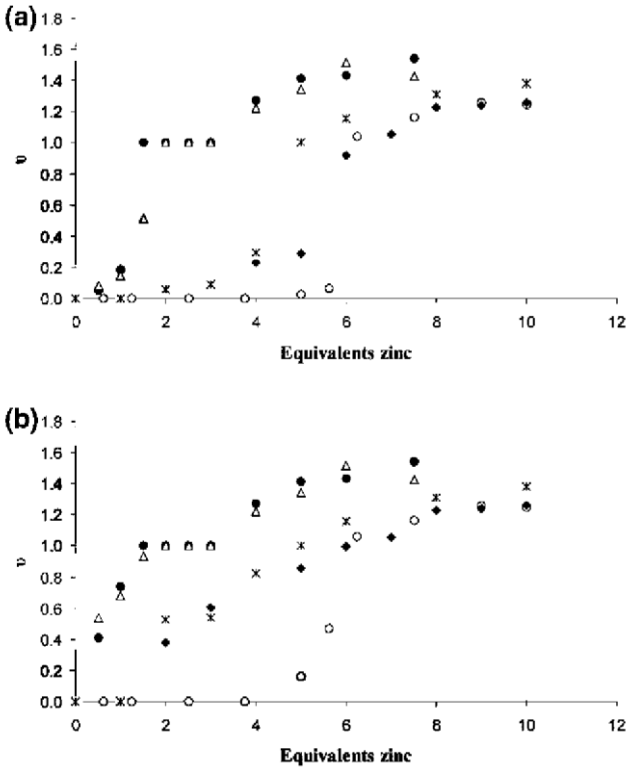

As reported by van den Bremer et al., nanoESI-MS can overestimate the contribution of the loosely packed conformation state of an apo-metallo-enzyme [20], a feature that may be explained by the increased exposure of hydrophobic residues enhancing the droplet surface affinity and, consequently, the ESI response. Moreover, highly charged ions have slightly higher detection efficiency. The enhanced ESI response of the less compact apo-enzyme will certainly affect the ratio of apo-enzyme to mono-zinc enzyme and, consequently, also the K_d. As the dissociation constant of CphA for the second zinc ion agrees well with the solution-based results, this indicates that the ionization efficiency of the apo-enzyme may indeed contribute to the discrepancy of the results for the first dissociation constant. Evidently, we need to introduce a correction factor for the difference in ionization efficiency between the two protein species E and EL when calculating K_d values. Following the reasoning described hereafter, we conclude that this factor is 12.5.

In titration methods such as the one described in this work, the concentration of protein (P) and protein-ligand complex (PL) in solution is assumed to be proportional to the observed intensities (I) in the mass spectrometer, following the equations

$$[P] = t_P \cdot I_P \qquad (3a)$$

$$[PL] = t_{PL} \cdot I_{PL} \qquad (3b)$$

The proportionality constants t_P and t_{PL} are the so-called transfer coefficients of P and PL. When L is much smaller in size than P, t_{PL} and t_P are nearly equal and the concentration ratio of [P]/[PL] is equal to the intensity ratio I_P/I_{PL}, an assumption which is only valid when there are no structural differences between the protein and the protein-ligand complex. To determine the relative transfer coefficient for apo-CphA and mono-zinc CphA, we followed the method described in [29]. In this method, equal amounts of two proteins are mixed and measured by ESI-MS. The ratio in intensity of the different species reflects the ratio of the transfer coefficients for these species. Using a mixture of equal amounts of (10 μM) apo-CphA and mono-zinc CphA, three independent measurements were performed and the ratio of the sum of the intensities of all charge states for both protein forms was calculated. It was found that apo-CphA has an ionization efficiency that is 12.5 times higher than the mono-zinc form.

The correction factor was used to recalculate the intensities of the apo-enzyme determined by the titration experiment. As such, a corrected plot could be constructed, which now gives lower $K_{d,1}$ values than previously calculated (Figure 5b and Table 1). Instead of 8 μM, $K_{d,1}$ for wild-type CphA is 1 μM or less, which is near the lower limit for the dissociation constant that can be determined using this plot.

Table 1: *Dissociation constants $K_{d,1}$ and $K_{d,2}$ for CphA mutants determined using nanoESI-MS. All values were derived using the plots from Figures 5 and 7*

CphA	**$K_{d,1}$ (μM) before correction**	**$K_{d,1}$ (μM) after correction**	**$K_{d,2}$ (μM)**
Wild-type	8	<1	50-55
K228Q	10	<1	50-55
N116H	50	50	>100
N220G	45	25	>100
N116H-N220G	40	25	>100
H118A	30	30	>100
H263S	30	20	>100
D120A	80	80	-
D120T	80	80	-

Figure 6: *Mass spectrum of mono-zinc CphA N116H-N220G after addition of 50 μM Zn^{2+} to the apo-enzyme. The peak labeled with an asterisk is a triply charged peptide impurity present in the sample.*

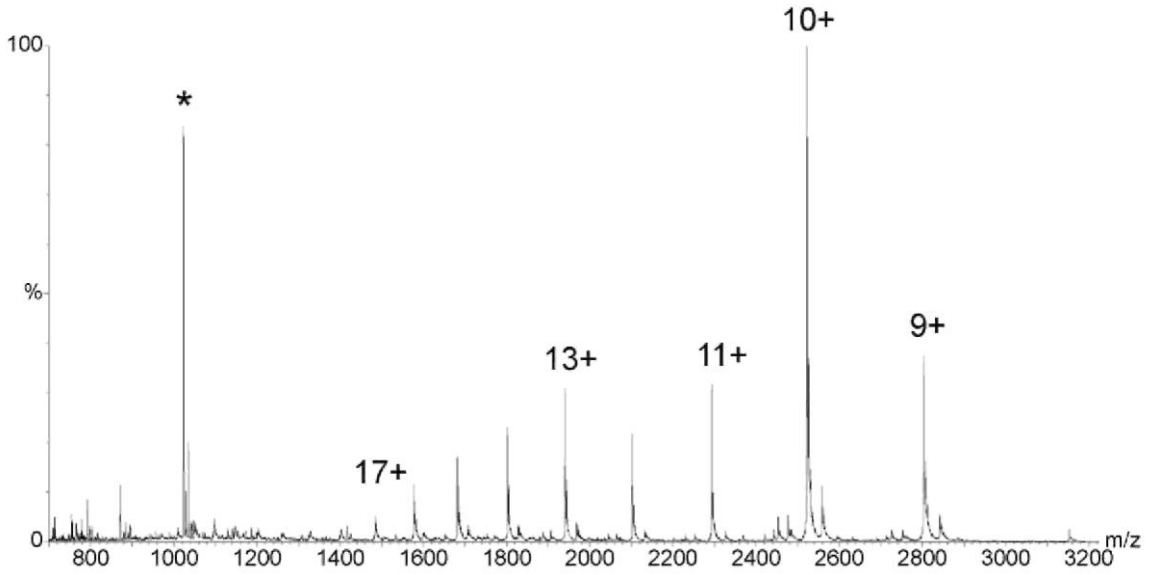

Zinc Titration of CphA Mutants

We applied the titration experiment to species of CphA in which key residues involved in Zn^{2+} binding were mutated. The mutant enzyme K228Q has a $K_{d,1}$ similar to that of the wild-type enzyme. K228 is not a zinc ligand in any of the two zinc binding sites and can therefore be expected to have an equal zinc affinity. This result thus shows that the method we used is reliable to deduce affinities of the mutant enzymes relative to the wild-type enzyme. The mutants N116H, N220G, and N116H-N220G are enzymes in which the B2 class motif (N116XH118XD120 ...H196...G219N220C221...H263) has been remodelled into a B1 class motif (H116XH118XD120... H196...G219G220C221...H263). All mutant enzymes have a decreased affinity for the first and the second zinc ion (Figure 5b). It was suggested by Vanhove et al. [30] that N116 is not involved in the binding of the second metal because N116S has a similar $K_{d,2}$ as the wild-type enzyme. N116H has been shown to have a broader substrate profile and a 5-fold increase in affinity compared to wild-type enzyme [30]. Our results, however, show a decreased affinity of N116H for zinc, and suggest a $K_{d,2}$ higher than 100 μM. More data points were not obtained because of decreasing ionization efficiency at higher zinc concentrations and to exclude the formation of nonspecific binding of zinc. $K_{d,1}$ of this mutant does not change remarkably after applying the correction factor, as seen from the steep slope of the curve between 5 and 7 equivalents of zinc. For N220G, a slightly higher affinity for the first zinc ion was recorded compared to N116H, but a similarly low affinity for the second zinc atom. Activity measurements for this mutant reported a $K_{d,2}$ for N220G of 86 μM with imipenem as substrate and of 110 μM with nitrocefin as substrate [22], values which agree with our mass spectrometric results. For the double mutant N116H-N220G a 5-fold decrease in $K_{d,2}$ was reported, compared to wild-type enzyme [22]. The apo-enzyme of N116H-N220G is unstable in ammonium acetate, as observed by the formation of a precipitate. When the enzyme binds a first zinc ion, the protein does not get refolded properly. The refolded mono-zinc species has charge states from 9+ to 17+ instead of 9+ to 11+, indicating only partial refolding of the protein (Figure 6). But even though the relative affinity of N116H-N220G, for the reasons mentioned above, is possibly incorrect, the double mutant still has a slightly higher zinc affinity than the single mutants N116H and N220G, as also reported in [22].

X-ray crystallography has revealed that D120 is a zinc ligand in the mono-zinc CphA, in contrast to the mono-nuclear enzymes of subclasses Bl and B3 [10]. The titration experiment indeed reveals that the mutant enzymes D120A and D120T have a decreased zinc affinity (Figure 7). D120A does not bind zinc unless at least 8 equivalents are added, and a completely mono-zinc enzyme is only detected when nine or 10 equivalents are added to CphA D120T and D120A, respectively. Even at these high zinc concentrations, the di-zinc enzyme is not formed. So, although it is the first binding site that is altered by the mutations, the second binding site appears to be affected as well. ICP-MS has revealed that these mutants do not form di-zinc enzyme in the presence of 100 μM Zn^{2+}, and that they have a very high decrease in activity towards imipenem (Christine Anne,

unpublished results). The mutants H118A and H263S have a similar affinity for zinc, with a $K_{d,1}$ around 30 μM and a $K_{d,2}$ higher than 100 μM. The latter value agrees well with the solution results (Christine Anne, unpublished results).

Figure 7: *Titration plot of number of zinc atoms per molecule of enzyme, ν, versus equivalent of zinc for wild-type CphA (filled circle), H118A (open square), H263S (filled triangle), D120A (open diamond), and D120T (asterisk) after applying the correction factor of 12.5 (see text).*

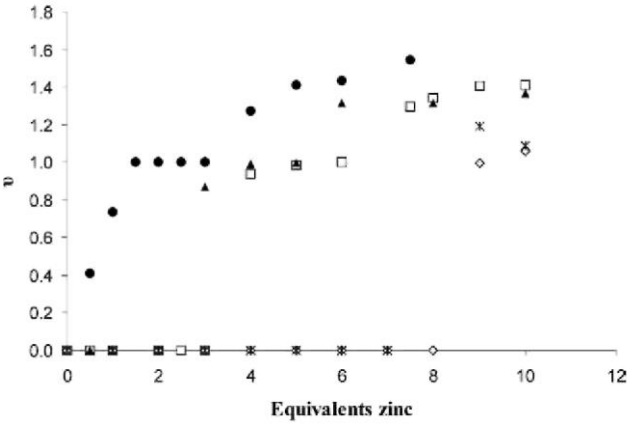

Conclusion

The metallo-β-lactamase CphA is an exceptional enzyme among the class B enzymes because of its narrow substrate profile and the inhibiting activity of the second zinc atom. Recently, the three-dimensional structure of CphA was determined, revealing that, unlike the other metallo-β-lactamases, the first zinc atom binds in the cysteine site, whereas the ligands of the potential histidine site are not well positioned for coordinating a zinc ion [10]. Several mutated enzymes were prepared to understand the mechanism towards carbapenems and the lack of activity towards penicillins and cephalosporins [22]. In the present work, the zinc affinity of some mutants was analyzed using nanoESI-MS. A chip-based nanoESI source was used, capable of analyzing the samples in an automatic infusion mode. The apo-enzyme of CphA was shown to exist in two different conformations: a less folded conformation with high charge states, and a compact conformation with low charge states. The removal of zinc by EDTA could be followed on-line after mixing enzyme and EDTA. Titration of the apo-enzyme with zinc results in a completely folded mono-zinc enzyme. Dissociation constants $K_{d,1}$ and $K_{d,2}$ for the first and second zinc atom are deduced from the titration curves. The values are listed in Table 1. The dissociation constant $K_{d,2}$ of the wild-type enzyme is comparable with the values reported from solution-based techniques. A correction factor based on the different ionization efficiency for the apo and mono-zinc form was determined and used to correct the calculated ratio of apo-enzyme to mono-zinc enzyme. As such, $K_{d,1}$ for the wild-type enzyme decreased nearly 10-fold and thus agreed better with results obtained in solution. For some mutant enzymes, the $K_{d,1}$ also decreased, but in fact remained quite high. It should be noted that a $K_{d,1}$ of 7 pM for the wild-type enzyme is too low to be determined using this method. The detection limit of the native CphA protein under our experimental conditions was 3 μM. For a protein with a single binding site, K_d is given by [E] x [L]/[EL]. If less than 3 μM CphA remains in solution at 1 equivalent of zinc (10 μM), then the lower limit for the dissociation constant is only slightly higher than 1 μM (K_d = (3 x 3)/7 = 1.3 μM).

In reference [22] the mutant enzymes were shown to exist as mono-zinc enzymes in buffer solutions with less than 0.4 μM Zn^{2+}. Therefore, the $K_{d,1}$values cannot be higher than 0.4 μM. At this stage, it is not clear to which extent the gas-phase stability of the complex reflects its solution stability. It should be noted that if some decomposition of the enzyme:Zn complex occurs in the gas-phase, this can result in a strong overestimation of $K_{d,1}$, especially when the $K_{d,1}$ values are very low. This is even enhanced by the fact that the ligand concentration is not much higher than the enzyme concentration. Therefore, the error on the calculation of the free zinc concentration at equilibrium can be very large, resulting in inaccurate dissociation constants. However, the relative affinities of the mutant CphA enzymes to the wild-type enzyme before and after data correction were found to be the same, and agree with those reported by Bebrone et al. [22], except for N116H and N116H-N220G. Our work also shows the importance of D120 in zinc coordination. It should be noted that the dissociation constants $K_{d,2}$ in [22] are determined by measuring the enzymatic activity of the mutants at increasing zinc concentrations. The method used in the present study is a direct measurement of the zinc affinity, which is not per se correlated to the enzymatic activity. Although several studies have successfully obtained

dissociation constants from gas-phase measurements, one can doubt whether ESI-MS will ever be routinely used to derive ligand affinities of proteins. In cases where no control sample or experiment can be performed or where there are no reference values available, the researcher should be careful about making conclusions solely on MS data.

Acknowledgments

This work is supported by the Federal Interuniversity Attraction Pole Program (project IUAP/V-P5/33), FRFC grants (2.4.508.01.F and 24.524.03), and the COBRA project (Sixth framework program of the European Union).

References

1. Majiduddin, F. K.; Materon, I. C; Palzkill, T. G. Molecular analysis of *β*-lactamase structure and function. *Int. J. Med. Microbiol.* 2002, *292*, 127-137.

2. Helfand, M. S.; Bonomo, R. A. *β*-lactamases: A survey of protein diversity. Curr. *Drug Targets Infect. Disord.* 2003, 3, 9-23.

3. Rice, L. B.; Bonomo, R. A. *β*-Lactamases: Which ones are clinically important? *Drug Resist. Update* 2000, 3, 178-189.

4. Galleni, M.; Lamotte-Brasseur, J.; Rossolini, M.; Spencer, J.; Dideberg, O.; Frère, J. M. Standard numbering scheme for class B *β*-lactamases. *Antimicrob. Agents Chemother.* 2001, 278, 23868-23873.

5. Carfi, A; Pares, S.; Duée, E.; Galleni, M.; Duez, C; Frère, J. M.; Dideberg, O. The 3-D structure of a zinc metallo-*β*-lactamase from *Bacillus cereus* reveals a new type of protein fold. *EMBO }.* 1995, *14*, 4914-4921.

6. Carfi, A.; Duée, E; Paul-Soto, R.; Galleni, M.; Frère, J. M.; Dideberg, O. X-ray structure of the ZnII *β*-lactamase from *Bacteroides fragilis* in an orthorhombic crystal form. Acta Crystallogr. D 1998, *54*, 45-57.

7. Garria-Sáez, I.; Mercuri, P. S.; Papamicael, C; Kahn, R.; Frère J. M.; Galleni, M.; Rossolini, G. M.; Dideberg, O. Three-dimensional structure of FEZ-1, a monomeric subclass B3 metallo-*β*-lactamase from *Fluorib-acter gormanii*, in native form and in complex with D-captopril. *J. Mol. Biol.* 2003, *325*, 651-660.

8. Ullah, J. H.; Walsh, T. R.; Taylor, I. A.; Emery, D. C; Verma, C. S.; Gamblin S. J.; Spencer, J. The crystal structure of the L1 metallo-*β*-lactamase from *Stenotrophomonas maltophilia* at 1.7 A resolution. *J. Mol. Biol.* 1998, *284*, 125-136.

9. Massidda, O.; Rossolini, G. M.; Satta, G. The *Aeromonas hydrophila* CphA gene: Molecular heterogeneity among class B metallo-*β*-lactamases. *J. Bacteriol.* 1991, *173*, 4611-4617.

10. Garau, G.; Bebrone, C.; Anne, C.; Galleni, M.; Frère, J. M.; Dideberg, O. A metallo-*β*-lactamase enzyme in action: Crystal structures of the monozinc carbapenemase CphA and its complex with biapenem. *J. Mol. Biol.* 2005, *345*, *785-795*.

11. Hernandez-Valladares, M.; Feliri, A.; Weber, G.; Adolph, H. W.; Zeppe-zauer, M.; Rossolini, G. M.; Amicosante, G.; Frère, J. M.; Galleni, M. Zn(II) dependence of the *Aeromonas hydrophila* AE036 metallo-*β*-lacta-mase activity and stability. *Biochemistry* 1997, *36*, 11534-11541.

12. Schultz, G. A.; Corso, T. N.; Prosser, S. J.; Zhang, S. A fully integrated monolithic microchip electrospray device for mass spectrometry. *Anal. Chem.* 2000, *72*, 4058-4063.

13. Benkestock, K.; Van Pelt, C. K.; Akerud, T.; Sterling, A.; Edlund, P.; Roeraarde, J. Automated nanoelectrospray mass spectrometry for pro-tein-ligand screening by noncovalent interaction applied to human H-FABP and A-FABP. *J. Biomol. Screen.* 2003, *8*, 247-256.

14. Zhang, S.; Van Pelt, C. K.; Wilson, D. B. Quantitative determination of noncovalent binding interactions using automated nanoelectrospray mass spectrometry. *Anal. Chem.* 2003, *75*, 3010-3018.

15. Keetch, C. A.; Hernandez, H.; Sterling, A.; Baumert, M.; Allen, M. H.; Robinson, C. V. Use of a microchip device coupled with mass spectrometry for ligand screening of a multi-protein target. *Anal. Chem.* 2003, *75*, 4937-4941.

16. De Vriendt, K.; Sandra, K.; Desmet, T.; Nerinckx, W.; Van Beeumen, J.; Devreese B. Evaluation of automated nanoelectrospray mass spectrometry in the determination of noncovalent protein-ligand complexes. *Rapid Commun. Mass Spectrom.* 2004, *24*, 3061-3067.

17. Urvoas, A.; Amekraz, B.; Moulin, C; Le Clainche, L.; Stöcklin, R.; Moutiez, M. Analysis of the metal-binding selectivity of the metal-lochaperone CopZ from *Enterococcus hirae* by electrospray ionization mass spectrometry. *Rapid Commun. Mass Spectrom.* 2003, *17*, 1889-1896.

18. Sudhir, P. R.; Wu, H. F.; Zhou, Z. C. An application of electrospray-ionization tandem mass spectrometer to probe the interaction of Ca^{2+}/Mg^{2+}/Zn^{2+} and Cl^{-} with gramicidin A. *Rapid Commun. Mass Spectrom.* 2005, *19*, 1517-1521.

19. Shindo, M.; Irie, K.; Fukuda, H.; Ohigashi, H. Analysis of noncovalent interaction between metal ions and the cysteine-rich domain of protein kinase Ceta by electrospray ionization mass spectrometry. *Bioorg. Med. Chem.* 2003, *11*, 5075-5082.

20. van den Bremer, E. T.; Jiskoot, W.; James, R.; Moore, G. R.; Kleanthous, C; Heck, A. J.; Maier, C. S. Probing metal ion binding and conformational properties of the colicin E9 endonuclease by electrospray ionization time-of-flight mass spectrometry. *Protein Sci.* 2002, *11*, 1738-1752.

21. van den Heuvel, R. H. H.; Gato, S.; Versluis, C; Gerbaux, P.; Kleanthous, C; Heck, A. J. R. Real-time monitoring of enzymatic DNA hydrolysis by electrospray ionization mass spectrometry. *Nucleic Acids Res.* 2005, *33*, e96.

22. Bebrone, C, Anne, C, De Vriendt, K., Devreese, B., Van Beeumen, J., Frère, J. M., Galleni, M. Dramatic broadening of the substrate profile of the *Aeromonas hydrophila* CphA metallo-*β*-lactamase by site-directed mutagenesis. *J. Biol. Chem.;* in press.

23. Cloupeau, M.; Prunet-Foch, B. Electrostatic spraying of liquids in cone-jet mode. *J. Electrostat.* 1989, *22*, 135-159.

24. Jackson, G. S.; Enke, C. G. The electrical equivalence of electrospray ionization mass spectrometry. *Anal. Chem.* 1999, *71*, 3777-3784.

25. Bicknell, R.; Emanuel, E. L.; Gagnon, J.; Waley, S. G. The production and molecular properties of the zinc *β*-lactamase of *Pseudomonas maltophilia* IID 1275. *Biochem. J* 1985, *229*, 791-797.

26. Mercuri, P. S.; Bouillenne, F.; Boschi, J.; Lamotte-Brasseur, G.; Amicosante, G.; Devreese, B.; Van Beeumen, J.; Frère, J. M.; Rossolini, G. M.; Galleni, M. Biochemical characterization of the FEZ-1 metallo-*β*-lacta-mase of *Legionella gormanii* ATCC 33297T produced in *Escherichia coli*. *Antimicrob. Agents Chemother.* 2001, *45*, 1254-1262.

27. Rossolini, G. M.; Franceschim, N.; Riccio, M. L.; Mercuri, P. S.; Perilli, M.; Galleni, M.; Frère, J. M.; Amicosante, G. Characterization and sequence of the *Chryseobacterium (Flavobacterium) meningosepticum* carbapenemase: A new molecular class B *β*-lactamase showing a broad substrate profile. *Biochem. J.* 1998, *332*, 145-152.

28. Laraki, N.; Franceschim, N.; Rossolini, G. M.; Santucci, P.; Meunier, C; De Pauw, E.; Amicosante, G.; Frère, J. M.; Galleni, M. Biochemical characterization of the *Pseudomonas aeruginosa* 101/1477 metallo *β*-lac-tamase IMP-1 produced by *Escherichia coli. Antimicrob. Agents Chemother.* 1999, *43*, 902-906.

29. Peschke, M.; Verkerk, U. H.; Kebarle, P. Features of the ESI mechanism that affect the observation of multiply charged noncovalent protein complexes and the determination of the association constant by the titration method. *J. Am. Soc. Mass Spectrom.* 2004, *15*, 1424-1434.

30. Vanhove, M.; Zakhem, M.; Devreese, B.; Francesschini, N.; Anne, C; Bebrone, C; Amicosante, G.; Rossolini, G. M.; Van Beeumen, J.; Frère, J. M.; Galleni, M. Role of Cys221 and Asnllô in the zinc binding sites of the *Aeromonas hydrophila* metallo-*β*-lactamase. *Cell. Mol. Life Sci.* 2003, *60*, 2501-2509.